# Supplementary Information for

# Does "Zero-Strain" Lithiated Spinel Serve as a Strain Retardant and Irreversible Phase Transition Regulator for Layered Oxide Cathode?

Authors: Zixin Wu,[a] Qizheng Zheng,[a] Guiyang Gao,[b] Jianhua Yin,[a] Leiyu Chen,[a] Yonglin Tang,[a] Yawen Yan,[a] Huan Huang,*[c] Yaru Qin,*[d] Xiaoxiao Kuai,*[ae] Yu Qiao*[ae] and Shi-Gang Sun[ae]

**Affiliations:**

[a] State Key Laboratory of Physical Chemistry of Solid Surfaces, Collaborative Innovation Center of Chemistry for Energy Materials (iChEM), Department of Chemistry, College of Chemistry and Chemical Engineering, Xiamen University, Xiamen, 361005, PR China

[b] State Key Laboratory of Physical Chemistry of Solid Surface, Fujian Key Laboratory of Surface and Interface Engineering for High Performance Materials, College of Materials, Xiamen University, Xiamen 361005, PR China

[c] The Institute of High Energy Physics, Chinese Academy of Sciences, Beijing 100190, PR China

[d] School of Chemistry and Chemical Engineering, Qinghai Minzu University, Xining 810007, PR China

[e] Fujian Science & Technology Innovation Laboratory for Energy Materials of China (Tan Kah Kee Innovation Laboratory), Xiamen 361005, PR China

* Correspondence to:

huanhuang@ihep.ac.cn (H. H.);

szdxqyr@126.com (Y. Q.);

kuaixiaoxiao@xmu.edu.cn (X. K.);

yuqiao@xmu.edu.cn (Y. Q.)

## Methods / Experimental Procedures

### $LiCoO_2$ (LCO) Powder Preparation

HT LCO: Lithium carbonate ($Li_2CO_3$, Energy Chemical, 99% metals basis) and cobalt carbonate ($CoCO_3$, Macklin, 99.99% metals basis) are uniformly mixed in a ratio of 1.05:1. The mixture is then subjected to a three-stage calcination in a muffle furnace in air: 1 hour at 500 ℃, 15 hours at 950 ℃, and another 15 hours at 720 ℃. The heating and cooling rate is 3℃/min. After each calcination step, the powder is ground and mixed in an agate mortar.

LT LCO: $Li_2CO_3$ and $CoCO_3$ (same kind as above) are uniformly mixed in a ratio of 1:1. The mixture is then calcinated in a muffle furnace in air for 6 days at 400 ℃.

Layered-spinel LCO: The above-mentioned LT LCO is then in a muffle furnace in air for 3 hours at 600 ℃. In addition, we synthesized various proportions of materials by adjusting temperature and time, as 600 °C 1h-LCO and 700 °C 1h-LCO shown in Figure 3c, d. The former is synthesized by calcination at 600 °C for 1 hour, and the latter is at 700 °C for 1 hour.

### Electrode Preparation

LCO material, Super-P and polyvinylidene fluoride (PVDF) comprise of the cathode slurry in a ratio of 90:5:5, with proper N-methyl pyrrolidone (NMP) as solvent. Then the slurry is homogeneously coated onto the carbon coated aluminum (Al) foil current collector by a scraper and dried in 110 ℃ for 12 hours in a vacuum oven. The material is finally cut into pieces of circle electrodes and each of them has a loading mass of the LCO materials about 3 $mg/cm^2$.

### Cell Assembly and Electrochemical Measurements

The LCO electrodes are assembled into a 2032-coin cell (Hohsen Corp.) in an Ar-filled glove box. The cathode and lithium foil anode (thickness, 50 nm) are separated by a polypropylene (PP) separator, which is impregnated with base electrolyte (1 M $LiPF_6$ in EC: DMC = 3:7, vol%). For coin cell, the galvanostatic electrochemical measurements are carried out under potential control using the battery tester system Neware battery cycle (CT-4008T-5V10mA-164, Shenzhen, China) at a constant temperature of 26 ℃. The LCO cells are in the range of 3.0-4.2/4.6 V (vs $Li/Li^+$), and respectively carried out at 0.1C (1C=200 mA/g). The $Li^+$

chemical diffusion coefficients ($D_{Li+}$) are detected using the GITT, which is performed at 0.1C for 1 hour of (dis)charging, followed by 8h of relaxation.

**X-ray Diffraction (XRD)**

In-situ XRD measurements are performed on a RIGAKU UtimalV diffractometer fitted with Cu-Kα X-rays (λ=1.5406 Å) radiation at a scan rate of 5°/min with scan range (2θ) of 10-60°. The Synchrotron powder XRD measurements are collected at the BL14W1 beamline of the Shanghai Synchrotron Radiation Facility. Corresponding structural illustrations of the structure are drawn using the program.[1] The refinement patterns are gained using GSAS II suite software.[2]

**Neutron powder diffraction (NPD)**

The neutron powder diffraction (NPD) measurements were performed on a time-offlight (TOF) neutron diffractometer GPPD (general purpose powder diffractometer) at the China Spallation Neutron Source (CSNS), Dongguan, China. The samples were loaded in 9.1 mm diameter vanadium cans, and neutron diffraction patterns were collected at room temperature with a wavelength band from 0.1 to 4.9 Å. The Rietveld refinement of the NPD was performed using the program GSAS-II.

**High Resolution Transmission Electron Microscopy (HR-TEM)**

The neutron powder diffraction (NPD) measurements were performed on a time-off-flight (TOF) neutron diffractometer GPPD (general purpose powder diffractometer) at the China Spallation Neutron Source (CSNS), Dongguan, China. The samples were loaded in 9.1 mm diameter vanadium cans, and neutron diffraction patterns were collected at room temperature with a wavelength band from 0.1 to 4.9 Å. The Rietveld refinement of the NPD was performed using the program GSAS-II.

**X-ray absorption spectroscopy (XAS)**

The Co and O ex-situ XAS spectra are collected in transmission mode at beamline BL14W1 of the of the Shanghai Synchrotron Radiation Facility (SSRF, Shanghai, China), which operates at 3.5 GeV in a "top-up" mode with an injection current of 220 mA. The data are treated using

the Athena program[3] for energy calibration and normalization.

**High Resolution Transmission Electron Microscopy (HR-TEM)**

HR-TEM images are obtained using a JEM-2100 (HR) electron micro-scope. For the HR-TEM observation, the original powders and cycled cathodes materials (current density is 20 mAh/g, cycle number is 1) are ultra-sounded in dimethoxy ethane (DME, Sigma Aldrich, 99%) solvent. After sufficient dispersion process, we employed a Cu mesh to harvest the dispersed particles for HR-TEM observation. Structure of graphite and other species are analyzed using Digital Micrograph (Gatan) software.

## Supplementary Discussion

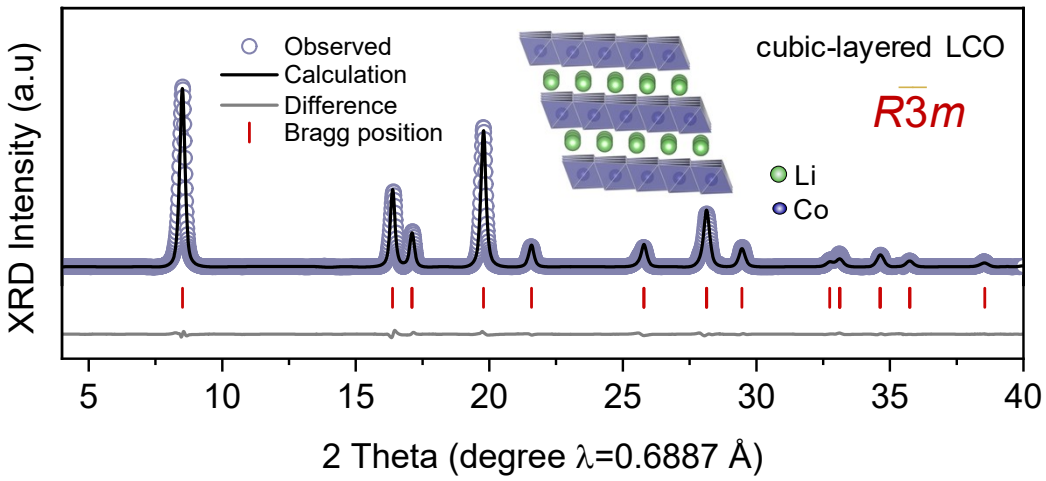


**Figure S1**. Refined synchrotron radiation XRD patterns of the pristine LT LCO with a cubic-layered structure.

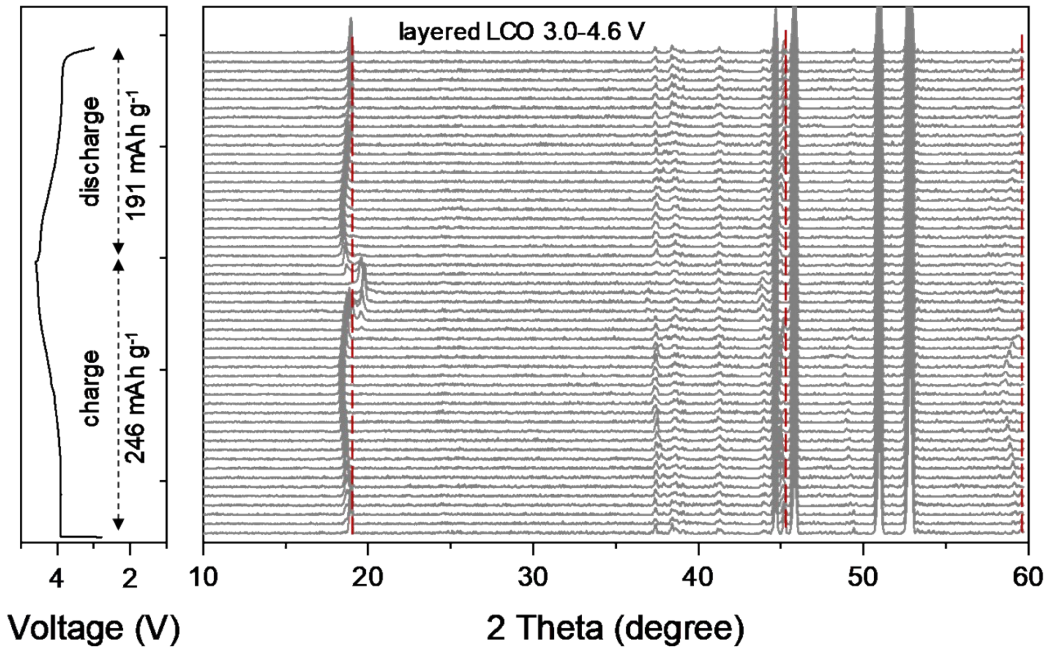


**Figure S2**. In-situ XRD patterns for the layered LCO and galvanostatic charge-discharge curve from 3 to 4.6 V (vs $Li/Li^+$).

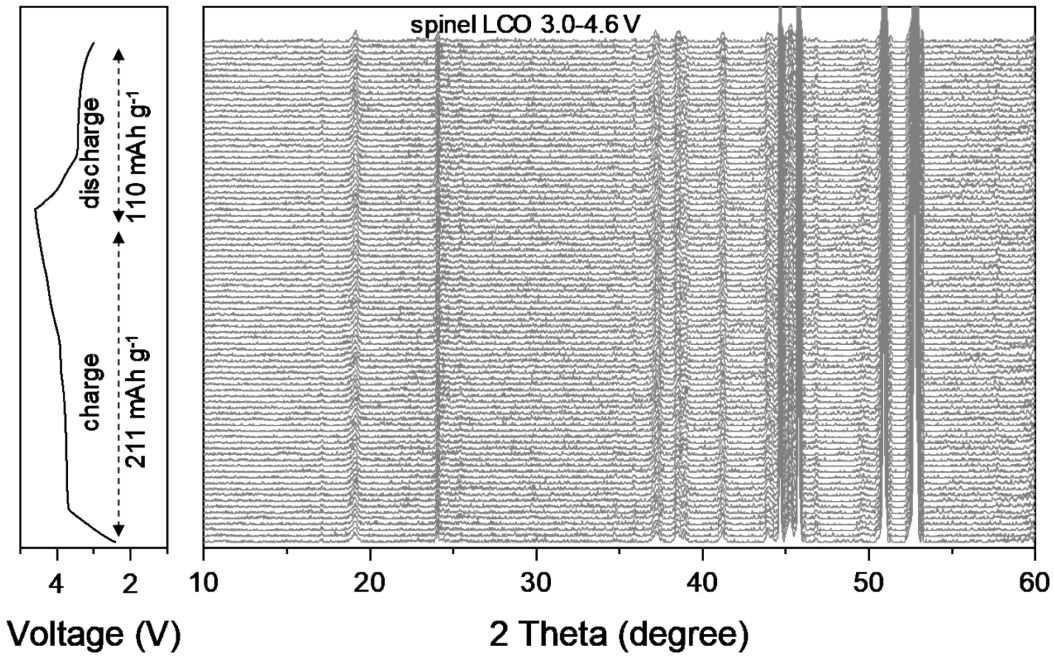


**Figure S3**. In-situ XRD patterns for the spinel LCO and galvanostatic charge-discharge curve from 3 to 4.6 V (vs $Li/Li^+$).

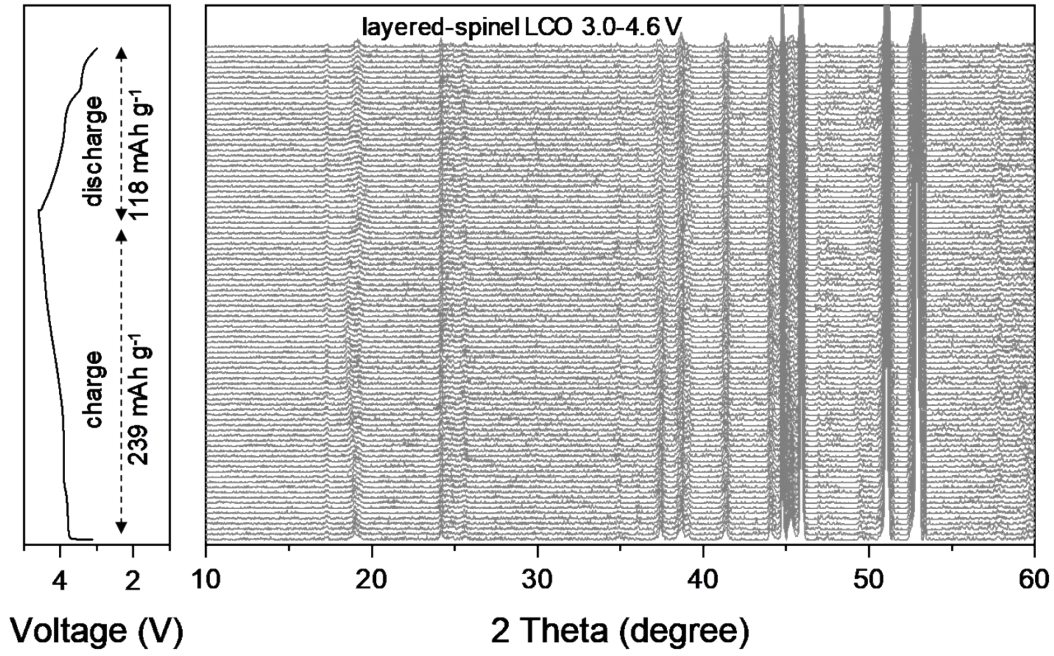


**Figure S4**. In-situ XRD patterns for the layered-spinel LCO and galvanostatic charge-discharge curve from 3 to 4.6 V (vs $Li/Li^+$).

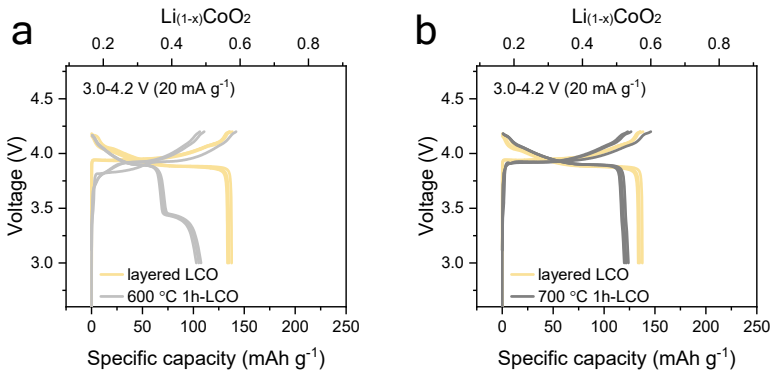


**Figure S5**. Charge-discharge profiles of (a) 600 °C 1h- LCO (spinel ratio > 10%) and (b) 700 °C 1h- LCO (spinel ratio < 10%) at 0.1 C, at voltage range of 3-4.2 V (vs $Li/Li^+$).

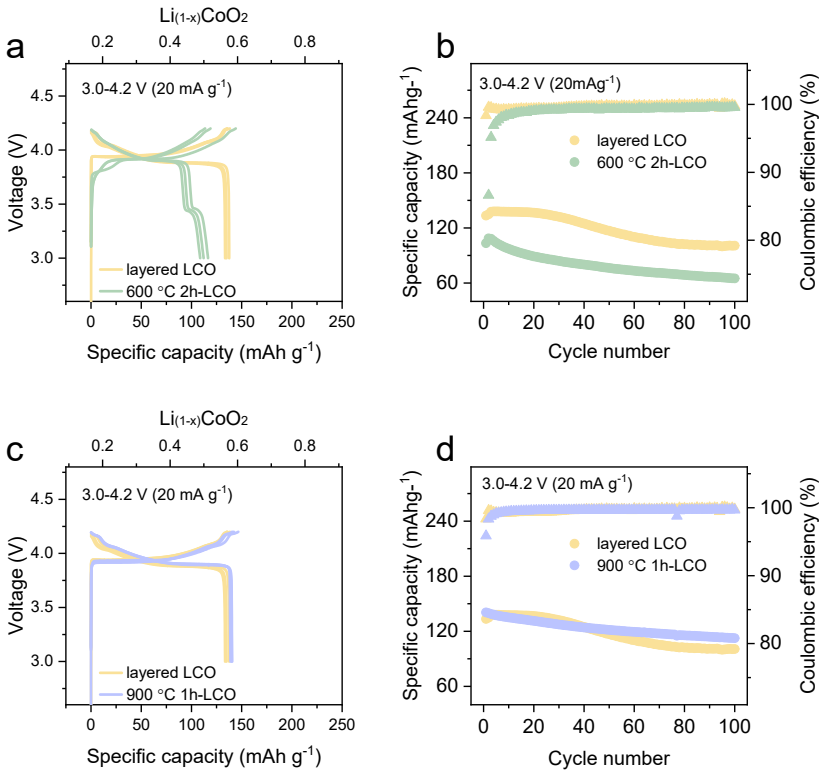


**Figure S6**. (a, c) Charge-discharge profiles of (a) 600 °C 2h- LCO and (c) 900 °C 1h- LCO, compared to the layered LCO, at 0.1 C at voltage range of 3-4.2 V (vs $Li/Li^+$). (b, d) Cycle performance of (b) 600 °C 2h- LCO and (d) 900 °C 1h- LCO , compared to the layered LCO, at 0.1 C at voltage range of 3-4.2 V (vs $Li/Li^+$).

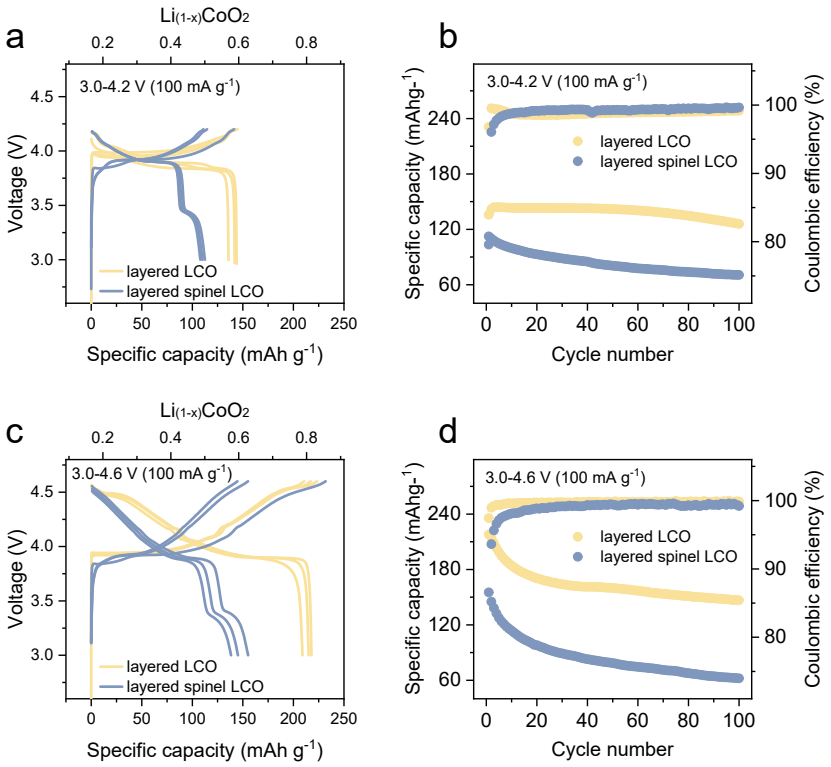


**Figure S7**. (a, c) Charge-discharge profiles of layered LCO and |layered-spinel LCO at 0.5 C, at voltage range of (a) 3-4.2 V and (c) 3-4.6 V (vs $Li/Li^+$). (b, d) Cycle performance of layered LCO and layered-spinel LCO at 0.5 C, at voltage range of (b) 3-4.2 V and (d) 3-4.6 V (vs $Li/Li^+$).

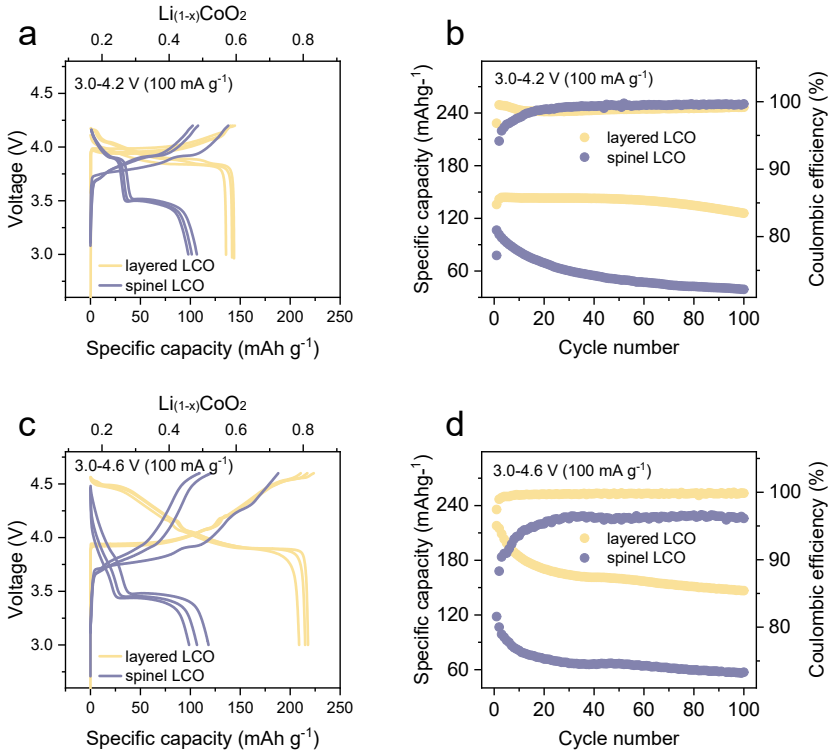


**Figure S8**. (a, c) Charge-discharge profiles of layered LCO and layered-spinel LCO at 0.5 C, at voltage range of (a) 3-4.2 V and (c) 3-4.6 V (vs $Li/Li^+$). (b, d) Cycle performance of layered LCO and spinel LCO at 0.5 C, at voltage range of (b) 3-4.2 V and (d) 3-4.6 V (vs $Li/Li^+$).

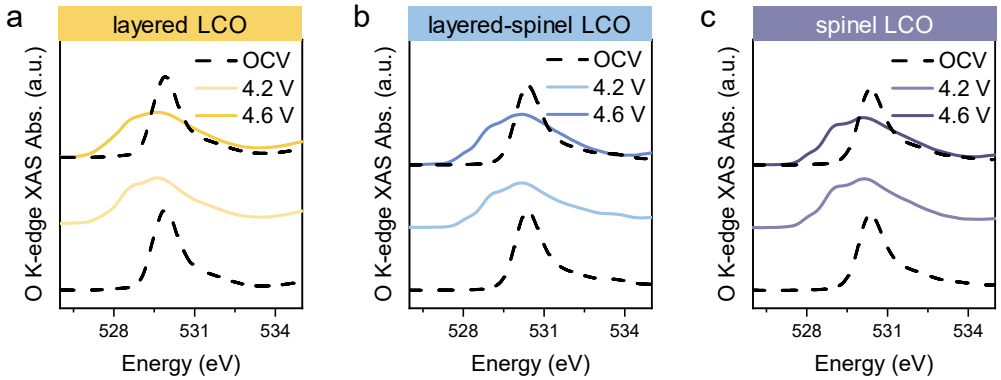


**Figure S9**. O K-edge XAS spectra (TEY mode) for (a) layered LCO, (b) layered-spinel LCO and (c) spinel LCO at states of pristine, 4.2 V, 4.6 V and 4.8 V (vs $Li/Li^+$). Based on the S8a figure, the main peak around 530 eV shifts to a lower energy, and two new signals appear around 528.5 and 527 eV as the voltage increases, indicating the oxidation of $Co^{3+}$. A similar situation is observed in the two graphs on the right, suggesting that the focus of this work is not on the Co-O covalent environment.

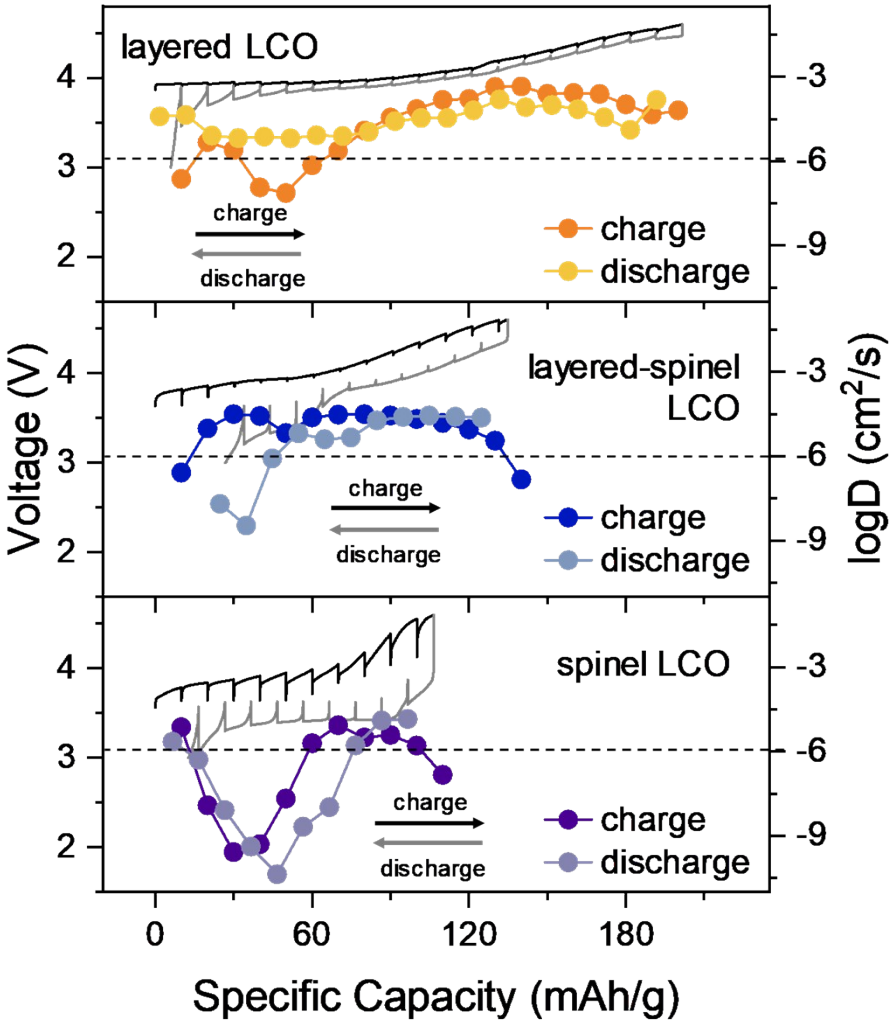


**Figure S10**. Diffusion coefficients ($D_{Li+}$, detected using GITT) and corresponding 1st cycle curves of LCO batteries. It is evident that the lithium ions transport rate of spinel LCO (LT LCO) is notably sluggish.

**Table S1.** Rietveld refinement results on the XRD pattern of HT LCO.

| R-3m layered | | $R_{wp}$=4.731% | | Chi2=1.04 | |
|---|---|---|---|---|---|
| a (Å) | 2.82468 | | | α (°) | 90 |
| c (Å) | 14.09851 | | | β (°) | 90 |
| c/a | 4.991 | | | γ (°) | 120 |
| Atom | Site | x | y | z | Occ |
| Li | 3a | 0.0000 | 0.0000 | 0.0000 | 1 |
| Co | 3b | 0.0000 | 0.0000 | 0.5000 | 1 |
| O | 6c | 0.0000 | 0.0000 | 0.24051 | 1 |

**Table S2.** Rietveld refinement results on the XRD pattern of LT LCO with a primary spinel structure.

| Two phases | | Rwp=2.176% | | Chi2=0.73 | |
|---|---|---|---|---|---|
| Phase 1 Fd-3m spinel | | α = β = γ (°) | | a (Å) | |
| 95.1 %wt | | 90 | | 8.00216 | |
| Atom | Site | x | y | z | Occ |
| Li1 | 16c | 0.0000 | 0.0000 | 0.0000 | 0.9747 |
| Li2 | 16d | 0.5000 | 0.5000 | 0.5000 | 0.0253 |
| Co1 | 16d | 0.5000 | 0.5000 | 0.5000 | 0.9747 |
| Co2 | 16c | 0.0000 | 0.0000 | 0.0000 | 0.0253 |
| O | 32e | 0.25718 | 0.25718 | 0.25718 | 1 |
| Phase 2 *Rm* layered | | | | 4.9 %wt | |
| a (Å) | 2.82468 | | | α (°) | 90 |
| c (Å) | 14.09851 | | | β (°) | 90 |
| c/a | 4.991 | | | γ (°) | 120 |
| Atom | Site | x | y | z | Occ |
| Li | 3a | 0.0000 | 0.0000 | 0.0000 | 1 |
| Co | 3b | 0.0000 | 0.0000 | 0.5000 | 1 |
| O | 6c | 0.0000 | 0.0000 | 0.24051 | 1 |

**Table S3.** Rietveld refinement results on the XRD pattern of layered-spinel LCO.

| Two phases | | | | Chi2=3.45 | |
|---|---|---|---|---|---|
| Phase 1 R-3m layered | | | | 89.7 %wt | |
| a (Å) | 2.82468 | | | α (°) | 90 |
| c (Å) | 14.09851 | | | β (°) | 90 |
| c/a | 4.991 | | | γ (°) | 120 |
| Atom | Site | x | y | z | Occ |
| Li | 3a | 0.0000 | 0.0000 | 0.0000 | 1 |
| Co | 3b | 0.0000 | 0.0000 | 0.5000 | 1 |
| O | 6c | 0.0000 | 0.0000 | 0.24051 | 1 |
| Phase 2 *Fdm* spinel | | α = β = γ (°) | | a (Å) | |
| 10.3 %wt | | 90 | | 8.00216 | |
| Atom | Site | x | y | z | Occ |
| Li1 | 16c | 0.0000 | 0.0000 | 0.0000 | 0.9747 |
| Li2 | 16d | 0.5000 | 0.5000 | 0.5000 | 0.0253 |
| Co1 | 16d | 0.5000 | 0.5000 | 0.5000 | 0.9747 |
| Co2 | 16c | 0.0000 | 0.0000 | 0.0000 | 0.0253 |
| O | 32e | 0.25718 | 0.25718 | 0.25718 | 1 |

**Table S4.** Rietveld refinement results on the XRD pattern of LT LCO with a primary cubic-layered structure.

| Two phases | | Rwp=1.811% | | Chi2=0.62 | |
|---|---|---|---|---|---|
| Phase 1 | R-3m cubic-layered | | | 95.1 %wt | |
| a (Å) | 2.82989 | | | α (°) | 90 |
| c (Å) | 13.87563 | | | β (°) | 90 |
| c/a | 4.903 | | | γ (°) | 120 |
| Atom | Site | x | y | z | Occ |
| Li1 | 3a | 0.0000 | 0.0000 | 0.0000 | 0.9892 |
| Li2 | 3b | 0.0000 | 0.0000 | 0.5000 | 0.0108 |
| Co1 | 3b | 0.0000 | 0.0000 | 0.5000 | 0.9892 |
| Co2 | 3a | 0.0000 | 0.0000 | 0.0000 | 0.0108 |
| O | 6c | 0.0000 | 0.0000 | 0.24178 | 1 |
| Phase 2 | R-3m layered | | | 4.9 %wt | |
| a (Å) | 2.82468 | | | α (°) | 90 |
| c (Å) | 14.09851 | | | β (°) | 90 |
| c/a | 4.991 | | | γ (°) | 120 |
| Atom | Site | x | y | z | Occ |
| Li | 3a | 0.0000 | 0.0000 | 0.0000 | 1 |
| Co | 3b | 0.0000 | 0.0000 | 0.5000 | 1 |
| O | 6c | 0.0000 | 0.0000 | 0.24051 | 1 |

**Table S5.** Rietveld refinement results on the NPD pattern of LT LCO with a primary spinel structure.

| Three phases | | | | Rwp=5.310% | |
|---|---|---|---|---|---|
| Phase 1 Fd-3m spinel | | α = β = γ (°) | | a (Å) | |
| 93.1 %wt | | 90 | | 8.00216 | |
| Atom | Site | x | y | z | Occ |
| Li1 | 16c | 0.0000 | 0.0000 | 0.0000 | 0.9747 |
| Li2 | 16d | 0.5000 | 0.5000 | 0.5000 | 0.0253 |
| Co1 | 16d | 0.5000 | 0.5000 | 0.5000 | 0.9747 |
| Co2 | 16c | 0.0000 | 0.0000 | 0.0000 | 0.0253 |
| O | 32e | 0.25718 | 0.25718 | 0.25718 | 1 |
| Phase 2 R-3m layered | | | | 4.8 %wt | |
| a (Å) | 2.82468 | | | α (°) | 90 |
| c (Å) | 14.09851 | | | β (°) | 90 |
| c/a | 4.991 | | | γ (°) | 120 |
| Atom | Site | x | y | z | Occ |
| Li | 3a | 0.0000 | 0.0000 | 0.0000 | 1 |
| Co | 3b | 0.0000 | 0.0000 | 0.5000 | 1 |
| O | 6c | 0.0000 | 0.0000 | 0.24051 | 1 |
| Phase3 $Li_2CO_3$ | | | | 2.1% | |

**Table S6.** Rietveld refinement results on the NPD pattern of LT LCO with a primary cubic-layered structure.

| Three phases | | | | $R_{wp}$=7.231% | |
|---|---|---|---|---|---|
| Phase 1 | R-3m cubic-layered | | | 93.1 %wt | |
| a (Å) | 2.82989 | | | α (°) | 90 |
| c (Å) | 13.87563 | | | β (°) | 90 |
| c/a | 4.903 | | | γ (°) | 120 |
| Atom | Site | x | y | z | Occ |
| Li1 | 3a | 0.0000 | 0.0000 | 0.0000 | 0.9892 |
| Li2 | 3b | 0.0000 | 0.0000 | 0.5000 | 0.0108 |
| Co1 | 3b | 0.0000 | 0.0000 | 0.5000 | 0.9892 |
| Co2 | 3a | 0.0000 | 0.0000 | 0.0000 | 0.0108 |
| O | 6c | 0.0000 | 0.0000 | 0.24178 | 1 |
| Phase 2 | R-3m layered | | | 4.8 %wt | |
| a (Å) | 2.82468 | | | α (°) | 90 |
| c (Å) | 14.09851 | | | β (°) | 90 |
| c/a | 4.991 | | | γ (°) | 120 |
| Atom | Site | x | y | z | Occ |
| Li | 3a | 0.0000 | 0.0000 | 0.0000 | 1 |
| Co | 3b | 0.0000 | 0.0000 | 0.5000 | 1 |
| O | 6c | 0.0000 | 0.0000 | 0.24051 | 1 |
| Phase3 | $Li_2CO_3$ | | | 2.1% | |

# Supplementary References

(1) Momma, K.; Izumi, F. VESTA 3for three-dimensional visualization of crystal, volumetric and morphology data. *J. Appl. Crystallogr.* **2011**, *44* (6), 1272-1276.

(2) Toby, B. H.; Von Dreele, R. B. GSAS-II: the genesis of a modern open-source all purpose crystallography software package. *J. Appl. Crystallogr.* **2013**, *46* (2), 544-549.

(3) Ravel, B.; Newville, M. ATHENA,ARTEMIS,HEPHAESTUS: data analysis for X-ray absorption spectroscopy usingIFEFFIT. *J. Synchrotron Radiat.* **2005**, *12* (4), 537-541.